Cellular Physiology and Biochemistry

Cell Physiol Biochem 2018;51:154-172
DOI: 10.1159/000495171
Published online: 15 November 2018
Accepted: 7 November 2018

Original Paper

Calcium Supplementation Enhanced Adipogenesis and Improved Glucose Homeostasis Through Activation of Camkii and PI3K/Akt Signaling Pathway in Porcine Bone Marrow Mesenchymal Stem Cells (pBMSCs) and Mice Fed High Fat Diet (HFD)

Fenglin Zhang[a,b] Jingjing Ye[a,b] Yingying Meng[a,b] Wei Ai[a,b] Han Su[a,b] Jisong Zheng[a,b] Fangfang Liu[a,b] Xiaotong Zhu[a,b] Lina Wang[a,b] Ping Gao[a,b] Gang Shu[a,b] Qingyan Jiang[a,b] Songbo Wang[a,b]

[a]Guangdong Provincial Key Laboratory of Animal Nutrition Control, College of Animal Science, South China Agricultural University, Guangzhou, [b]National Engineering Research Center for Breeding Swine Industry and ALLTECH-SCAU Animal Nutrition Control Research Alliance, South China Agricultural University, Guangzhou, China

Key Words
Calcium supplementation • Adipogenesis • Glucose homeostasis • CaMKII • PI3K/Akt

Abstract
Background/Aims: It has been implicated that calcium supplementation is involved in reducing body weight/fat and improving glucose homeostasis. However, the underlying mechanisms are still not fully understood. Here, we investigated the effects of calcium supplementation on adipogenesis and glucose homeostasis in porcine bone marrow mesenchymal stem cells (pBMSCs) and high fat diet (HFD)-fed mice and explored the involved signaling pathways. ***Methods:*** *In vitro*, pBMSCs were treated with 4 mM extracellular calcium ($[Ca^{2+}]_o$) and/or 1 μM nifedipine, 0.1 μM BAPTA-AM, 1 μM KN-93, 50 nM wortmannin for 10 days. The intracellular calcium ($[Ca^{2+}]_i$) levels were measured using Fluo 3-AM by flow cytometry. The adipogenic differentiation of pBMSCs was determined by Oil Red-O staining and triglyceride assay. The expression of marker genes involved in adipogenesis (peroxisome proliferator activated receptor γ (PPARγ) and CCAAT/enhancer binding protein α (C/EBPα)) and glucose uptake (glucose transporter 4 (GLUT4)), as well as the activation of Ca^{2+}/calmodulin-dependent

F. Zhang and J. Ye contributed equally to this work.

Songbo Wang
Guangdong Provincial Key Laboratory of Animal Nutrition Control, College of Animal Science, South China Agricultural University, Guangzhou 510642 (China)
Tel. +862085284901, E-Mail songbowang@scau.edu.cn

protein kinase II (CaMKII) and PI3K/Akt-FoxO1/AS160 signaling pathways were determined by Western blotting. Glucose uptake and utilization were examined using 2-NBDG assay and glucose content assay, respectively. *In vivo*, C57BL/6J male mice were fed a HFD (containing 1.2% calcium) without or with 0.6% (w/w) calcium chloride in drinking water for 13 weeks. The adipogenesis, glucose homeostasis and the involvement of CaMKII and PI3K/Akt signaling pathway were also assessed. ***Results:*** *In vitro*, $[Ca^{2+}]_o$ stimulated pBMSCs adipogenesis by increasing $[Ca^{2+}]_i$ level and activating CaMKII and PI3K/Akt-FoxO1 pathways. In addition, $[Ca^{2+}]_o$ promoted glucose uptake/utilization by enhancing AS160 phosphorylation, GLUT4 expression and translocation. However, the stimulating effects of $[Ca^{2+}]_o$ on pBMSCs adipogenesis and glucose uptake/utilization were abolished by L-VGCC blocker Nifedipine, $[Ca^{2+}]_i$ chelator BAPTA-AM, CaMKII inhibitor KN-93, or PI3K inhibitor Wortmannin. *In vivo*, calcium supplementation decreased body weight and fat content, increased adipocyte number, and improved glucose homeostasis, with elevated PPARγ and GLUT4 expression and PI3K/Akt activation in iWAT. ***Conclusion:*** calcium supplementation enhanced adipogenesis and glucose uptake in pBMSCs, which was coincident with the increased adipocyte number and improved glucose homeostasis in HFD-fed mice, and was associated with activation of CaMKII and PI3K/Akt-FoxO1/AS160 pathways. These data provided a broader understanding of the mechanisms underlying calcium-induced body weight/fat loss and glycemic control.

Introduction

Obesity, a major risk factor for the development of insulin resistance, type 2 diabetes and cardiovascular diseases, has been a pandemic and serious public health challenge worldwide [1]. Although the expanded fat mass can result from the increased adipocyte size (hypertrophy) and/or increased adipocyte number (hyperplasia or adipogenesis) [2], it has been demonstrated that hypertrophic adipose expansion is associated with obesity and impaired insulin sensitivity while hyperplasic adipose expansion or adipogenesis is linked to anti-obesity and improved insulin sensitivity [3-5]. Thus, stimulation of adipocyte hyperplasia or adipogenesis may contribute to prevention of obesity, insulin resistance and type 2 diabetes.

Adipogenesis is a complicated process which includes the commitment of mesenchymal stem cells (MSCs) to the adipocyte lineage (preadipocytes) and the terminal differentiation of preadipocytes to mature adipocytes. This process is tightly regulated by various signaling molecules and several key adipogenic transcription factors such as peroxisome proliferator activated receptor γ (PPARγ) and CCAAT/enhancer binding protein α (C/EBPα) [6]. During adipogenesis, triglyceride (TG) is accumulated in the adipocytes through lipogenesis [7]. The de novo lipogenesis in adipose tissue is affected by the expression, translocation of glucose transporter 4 (GLUT4) and glucose uptake, and exerts beneficial effects on insulin sensitivity [4, 8]. Pigs have been widely used as valuable models in biomedical research because of their similar structure and function to those of humans [9]. Thus, the porcine bone marrow MSCs (pBMSCs) were selected for the *in vitro* studies in the present study.

It has been demonstrated that calcium is involved in the adipogenesis of 3T3-L1 cells [10], human preadipocytes [11], and mice BMSCs [12]. However, calcium has quite different, even opposite effects on adipogenesis, depending upon the various cell types. In addition, calcium also plays an important role in regulating glucose uptake in the isolated working rat heart [13], mice skeletal muscle [14], and 3T3-L1 cells [15]. Moreover, dietary calcium has been confirmed to elicit beneficial effects on body weight/fat reduction and glycemic control [16-18]. Although the increase of fat oxidation and fecal fat excretion [19], the elevation of adipose tissue apoptosis [20], and the gut microbiota [16, 21] have been implicated to be partly involved, the mechanisms by which calcium modulates body weight/fat and glucose homeostasis are still not fully understood.

Thus, this study was designed to investigate the effects of calcium supplementation on adipogenesis and glucose homeostasis in pBMSCs and mice fed HFD and explore the

signaling pathways involved in this process. Our data showed that calcium supplementation enhanced adipogenesis and glucose uptake in pBMSCs, and increased adipocyte number, improved glucose tolerance and insulin sensitivity in HFD-fed mice through activation of Ca^{2+}/calmodulin-dependent protein kinase II (CaMKII) and PI3K/Akt signaling pathway, which might contribute to the reduction of body weight/fat and improvement of glucose homeostasis.

Materials and Methods

Chemicals and antibodies

Calcium acetate, calcium chloride, Nifedipine (a selective inhibitor of L-type voltage-gated calcium channels, L-VGCC), calcium indicator Fluo-3 AM, BAPTA-AM (a selective chelator of intracellular calcium), insulin, dexamethasone, oleic acid, octanoic acid, KN-93 (a CaMKII inhibitor), 2-NBDG (a fluorescent glucose analogue) and Oil Red O were purchased from Sigma-Aldrich. Wortmannin (WT, a PI3K/Akt inhibitor) was purchased from Beyotime Biotechnology. DMEM/F12 and fetal bovine serum (FBS) were purchased from Gibco BRL. Antibodies against PPARγ, C/EBPα, phospho-PI3K p85α (Tyr508), Akt, phospho-Akt (Thr308), FoxO1 and phospho-FoxO1 (Ser256), AS160, phospho-AS160 (Thr642) were purchased from Cell Signaling Technology Inc. Antibodies against β-actin, GLUT4, PI3K p85α and CaMKII were purchased from Bioss Inc. Antibodies against aP2 and phospho-CaMKII (Thr286) were purchased from Santa Cruz Biotechnology, Inc..

Cell culture and treatment

pBMSCs were isolated and purified from the bone marrow of postnatal Landrace pigs aged of 5 to 7 days as previously described [22]. The purified pBMSCs were seeded in a 6-well plate with density of 300, 000 cells/well and cultured in DMEM/F12 medium (containing 1 mM calcium) with 10% (v/v) FBS. Two days post-confluence, cells were switched to differentiation medium (DMEM/F12 supplemented with 50 nM insulin, 50 nM dexamethasone, 50 μM oleic acid，0.5 mM octanoic acid, 5% FBS, 100 U/mL of penicillin sodium and 100 μg/L of streptomycin sulfate). During the adipogenic differentiation, the pBMSCs were treated with various concentrations (1, 2, 4 mM) of extracellular calcium ($[Ca^{2+}]_o$) for 10 days to investigate the effects of $[Ca^{2+}]_o$ on pBMSCs adipogenesis. In addition, the cells were treated with 4 mM $[Ca^{2+}]_o$ and/or 1 μM nifedipine, 0.1 μM BAPTA-AM, 1 μM KN-93, 50 nM WT for 10 days to explore the role of L-VGCC, intracellular calcium, CaMKII and PI3K/Akt signaling pathway in $[Ca^{2+}]_o$-mediated adipogenesis and glucose uptake in pBMSCs, respectively.

Oil Red-O staining and Triglyceride (TG) assay

Lipid accumulation and TG contents in the differentiated pBMSCs were determined by Oil Red O staining and a TG assay kit (Applygen Technologies Inc, China) as previously described [5, 23].

Glucose uptake and utilization assay

Glucose uptake into the differentiated pBMSCs was measured using 2-NBDG as previously described with a Synergy 2 Multi-Mode Reader (Bio-Tek, USA) [5]. Glucose utilization of the differentiated pBMSCs were determined using glucose content assay kit (Applygen Technologies Inc, China) as previously described [24].

Measurements of $[Ca^{2+}]$

The $[Ca^{2+}]_i$ levels of pBMSCs were measured using Fluo 3-AM by flow cytometry as previously described [25].

Animal and in vivo study

Twenty-eight C57BL/6J male mice (4-week-old) were purchased from Guangdong Medical Laboratory Animal Center and housed in environmentally controlled rooms on a 12-h light-dark cycle (light from 08:00 to 20:00) with free access to food and water. After 5 days of acclimation, the mice were randomly divided into the HFD group (n=15) and HFD+Ca^{2+}group (n=13) and were fed a HFD (45% energy from fat, containing 1.2% calcium) without or with 0.6% (w/w) calcium chloride in drinking water, respectively. The body weight

and food intake were recorded weekly. After treatment for 13 weeks, the body fat content and body fat distribution were determined by using Small Animal Body Composition Analysis and Imaging System NMR Analyzer (MesoQMR23-060H, Niumag Corporation, Shanghai, China). The mice were sacrificed by carbon dioxide anesthesia. The blood was collected for determination of blood glucose and serum insulin levels. Meanwhile, the inguinal white adipose tissue (iWAT) and epididymal WAT (eWAT) were collected, weighed, and used for further analysis. All animal experiments were conducted with the permission number of SYXK (Guangdong) 2014-0136, and animal care procedures were performed in accordance with the guidelines for the care and use of animals approved by The Animal Ethics Committee of South China Agricultural University.

H&E staining, adipocyte diameter and adipocyte number analysis

The paraffin-embedded iWAT sections were stained with H&E as previously described [23]. Adipocyte diameter and adipocyte number analysis was performed as previously described [5].

Oral glucose tolerance test (OGTT) and intraperitoneal insulin tolerance test (ITT)

After the mice were treated for 10 weeks, OGTT and ITT were performed as previously described [5].

Western blot analysis

The protein of pBMSCs and iWAT was extracted and Western blot analysis was performed as previously described [25]. We used anti-PPARγ (1:2000), anti-C/EBPα (1:2000), anti-aP2 (1:500), anti-GLUT4 (1:1000), anti-CaMKII (1:2000), anti-p-CaMKII (1:500), anti-PI3K (1:2000), anti-p-PI3K (1:2000), anti-Akt (1:2000), anti-p-Akt (1:2000), anti-FoxO1 (1:2000), anti-p-FoxO1 (1:2000), anti-AS160 (1:2000), anti-p-AS160 (1:2000), anti-β-actin (1:2000), and anti-Caveolin-1 (1:2000). Densitometry analysis was perform using image J software.

Statistical Analysis

All data are presented as means ± standard error of the mean (S.E.M.). Statistical analysis was performed using SigmaPlot 12.5 (Systat Software, Inc., San Jose, CA). Differences between means were determined using two-tailed Student's t-test and a confidence level of $P < 0.05$ was considered to be statistically significant.

Results

L-VGCC blocker abolished the $[Ca^{2+}]_o$-induced elevation of $[Ca^{2+}]_i$ and stimulation of pBMSCs adipogenesis

The results of Oil Red O staining (Fig. 1A) and TG content assay (Fig. 1B) demonstrated that $[Ca^{2+}]_o$ significantly stimulated pBMSCs adipogenesis, with elevated protein expression of adipogenic marker genes such as PPARγ, C/EBPα, and aP2 (Fig. 1C, D). Meanwhile, we found that the $[Ca^{2+}]_i$, indicated as relative fluorescence intensity, was significantly elevated by 4 mM $[Ca^{2+}]_o$ and that the elevation of $[Ca^{2+}]_i$ in response to $[Ca^{2+}]_o$ was reversed by L-VGCC blocker Nifedipine (Fig. 2A, B). Furthermore, Nifedipine completely abolished the promotion of lipid accumulation induced by 4 mM $[Ca^{2+}]_o$ in pBMSCs (Fig. 2C, D). In agreement, the $[Ca^{2+}]_o$-induced increase of PPARγ, CEBPα, and aP2 expression was eliminated by Nifedipine (Fig. 2E, F). These results strongly suggested that calcium influx though L-VGCC was involved in $[Ca^{2+}]_o$-induced elevation of $[Ca^{2+}]_i$ and stimulation of pBMSCs adipogenesis.

Chelation of $[Ca^{2+}]_i$ prevented the $[Ca^{2+}]_o$-stimulated pBMSCs adipogenesis

BAPTA-AM, a membrane-permeable $[Ca^{2+}]_i$ chelator, was used to elucidate the association between the elevation of $[Ca^{2+}]_i$ and the $[Ca^{2+}]_o$-stimulated pBMSCs adipogenesis. As expected, the elevation of $[Ca^{2+}]_i$ in response to 4 mM $[Ca^{2+}]_o$ was absolutely eliminated by 0.1 μM BAPTA-AM (Fig. 3A, B). Meanwhile, $[Ca^{2+}]_i$ chelation completely abolished the promotion of lipid accumulation induced by $[Ca^{2+}]_o$ in pBMSCs (Fig. 3C, D). In addition, the stimulation of PPARγ, C/EBPα, and aP2 protein expression induced by $[Ca^{2+}]_o$ was totally

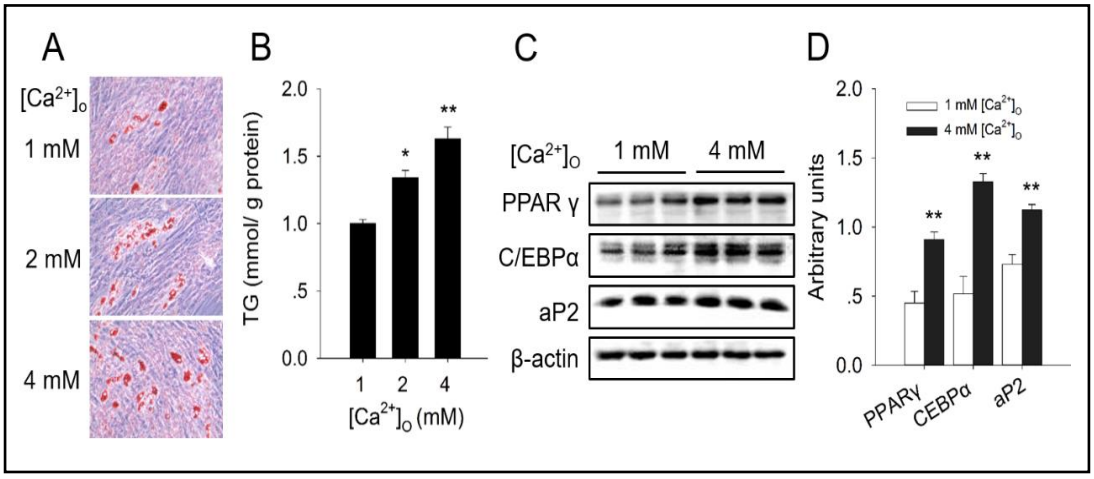

Fig. 1. $[Ca^{2+}]_o$ promoted the adipogenesis of pBMSCs. A and B: Oil Red O staining (A) and triglyceride (TG) contents assay (B) were conducted in the differentiated pBMSCs treated with various concentrations (1, 2 and 4 mmol/L) of $[Ca^{2+}]_o$ after 10-day adipogenic differentiation. Microscopic pictures were taken on day 10 with × 100 magnification. The TG content was normalized to total protein concentration. C: Western blot analysis of adipogenic marker genes (PPARγ, C/EBPα and aP2) in the differentiated pBMSCs after 10-day adipogenic differentiation, and β-actin was used as a loading control. D: Mean ± SEM of immunoblotting bands of PPARγ, C/EBPα and aP2, and the intensities of the bands were expressed as the arbitrary units. ** $P<0.01$ versus 1 mmol/L $[Ca^{2+}]_o$ group (control).

prevented by BAPTA-AM (Fig. 3E, F). These results demonstrated that chelation of $[Ca^{2+}]_i$ fully reversed the elevation of $[Ca^{2+}]_i$ and stimulation of pBMSCs adipogenesis induced by $[Ca^{2+}]_o$, suggesting the association of increased $[Ca^{2+}]_i$ with $[Ca^{2+}]_o$-stimulated pBMSCs adipogenesis.

Activation of CaMKII was involved in the $[Ca^{2+}]_o$-stimulated pBMSCs adipogenesis

As CaMKII is an important downstream target of $[Ca^{2+}]_i$, we further explored the role of CaMKII in $[Ca^{2+}]_o$-stimulated pBMSCs adipogenesis. We found that $[Ca^{2+}]_o$ led to significant increase of the p-CaMKII/CaMKII ratio, suggesting the activation of CaMKII. Interestingly, the $[Ca^{2+}]_o$-induced activation of CaMKII was reversed by Nifedipine and BAPTA-AM (Fig. 4A-D), indicating that $[Ca^{2+}]_o$ activated CaMKII through calcium influx via L-VGCC and elevation of $[Ca^{2+}]_i$. In addition, inhibition of CaMKII with 1 μM KN-93 completely abolished the increase of lipid accumulation and TG contents (Fig. 4E, F), and the elevation of PPARγ, CEBPα and aP2 expression (Fig. 4G, H) induced by $[Ca^{2+}]_o$. These findings indicated that the activation of CaMKII signaling pathway was involved in $[Ca^{2+}]_o$-stimulated pBMSCs adipogenesis.

$[Ca^{2+}]_o$-induced enhancement of PI3K/Akt signaling pathway depended on L-VGCC, $[Ca^{2+}]_i$ and CaMKII

We further assessed the possible role of PI3K/Akt signaling pathway in $[Ca^{2+}]_o$-stimulated pBMSCs adipogenesis. As shown in Fig. 5, $[Ca^{2+}]_o$ significantly increased the ratios of p-PI3K/PI3K, p-Akt/Akt, suggesting the activation of the PI3K/Akt signaling pathway. Meanwhile, the phosphorylation level of FoxO1, the downstream target of PI3K/Akt, was also elevated. However, the activation of PI3K/Akt-FoxO1 pathway was totally reversed by Nifedipine, BAPTA-AM and KN-93. These results suggested that $[Ca^{2+}]_o$ enhanced the PI3K/Akt-FoxO1 signaling pathway during pBMSCs adipogenesis and this enhancement was dependent on calcium influx via L-VGCC, elevation of $[Ca^{2+}]_i$ and activation of CaMKII.

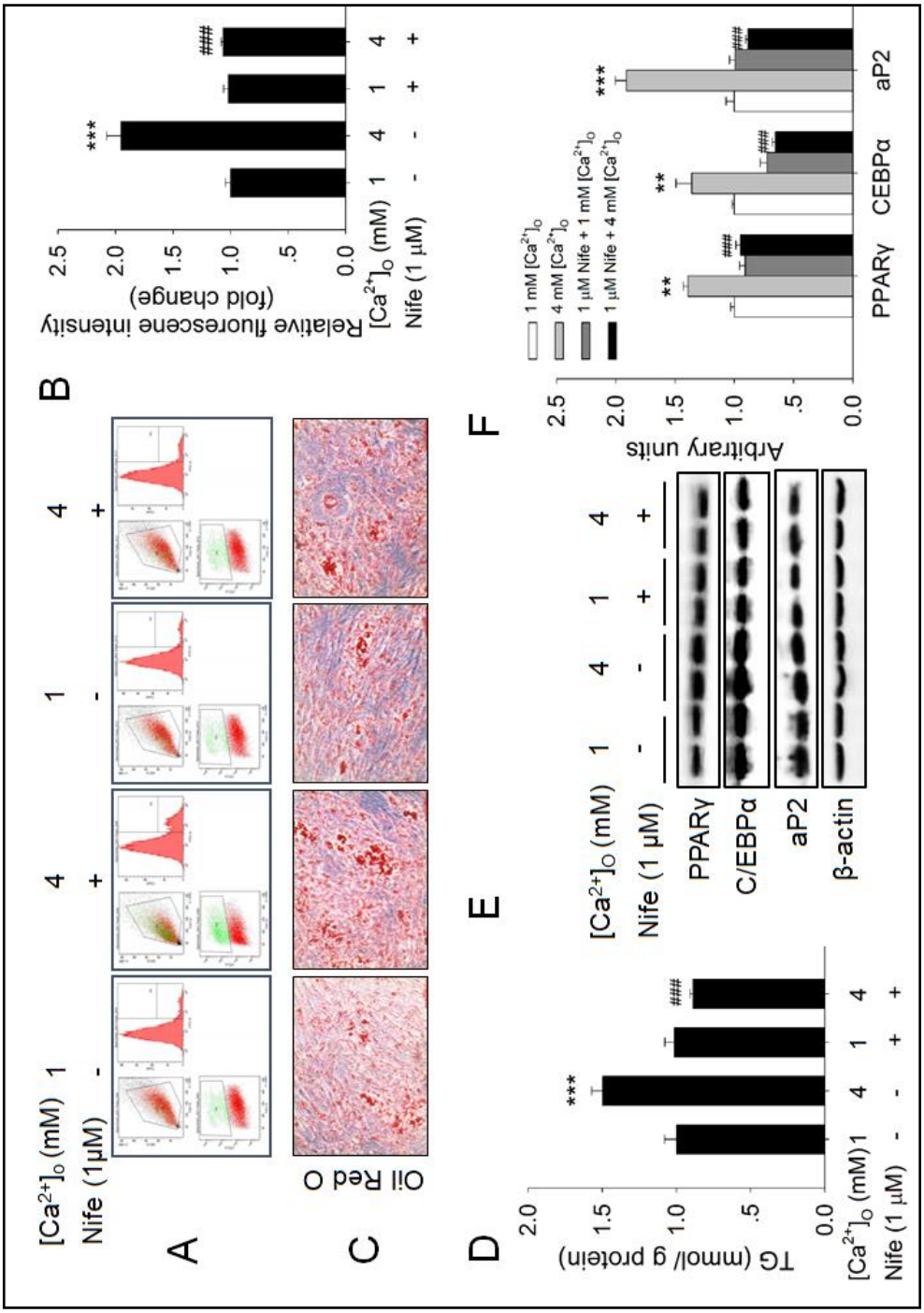

Fig. 2. L-VGCC blocker abolished the $[Ca^{2+}]_o$-induced elevation of $[Ca^{2+}]_i$ and stimulation of pBMSCs adipogenesis. A: $[Ca^{2+}]_i$ was analyzed by flow cytometry in the presence of 4 mM $[Ca^{2+}]_o$ and/or 1 μM Nifedipine (Nife). In the upper left image, the x axis is the forward scatter area (FSC-A) and the y axis is the side scatter area (SSC-A). In the bottom left image, the x axis is the forward scatter area (FSC-A) and the y axis is fluoresceinisothiocyanate area (FITC-A). In the upper right image, the x axis is fluorescein isothiocyanate area (FITC-A) and the y axis is the cell count according to the different fluorescence displayed by the x-axis. B: The relative FITC fluorescence intensity of gated positive cells. C and D: Oil Red O staining (C) and TG contents assay (D) were conducted in the differentiated pBMSCs after 10-day adipogenic differentiation. E: Western blot analysis of PPARγ, C/EBPα and aP2 in the differentiated pBMSCs after 10-day adipogenic differentiation, and β-actin was used as a loading control. F: Mean ± SEM of immunoblotting bands and the intensities of the bands were expressed as the arbitrary units. ** P<0.01 and ***P<0.001 versus 1 mM $[Ca^{2+}]_o$ group (control), ###P<0.001 versus 4 mM $[Ca^{2+}]_o$ group.

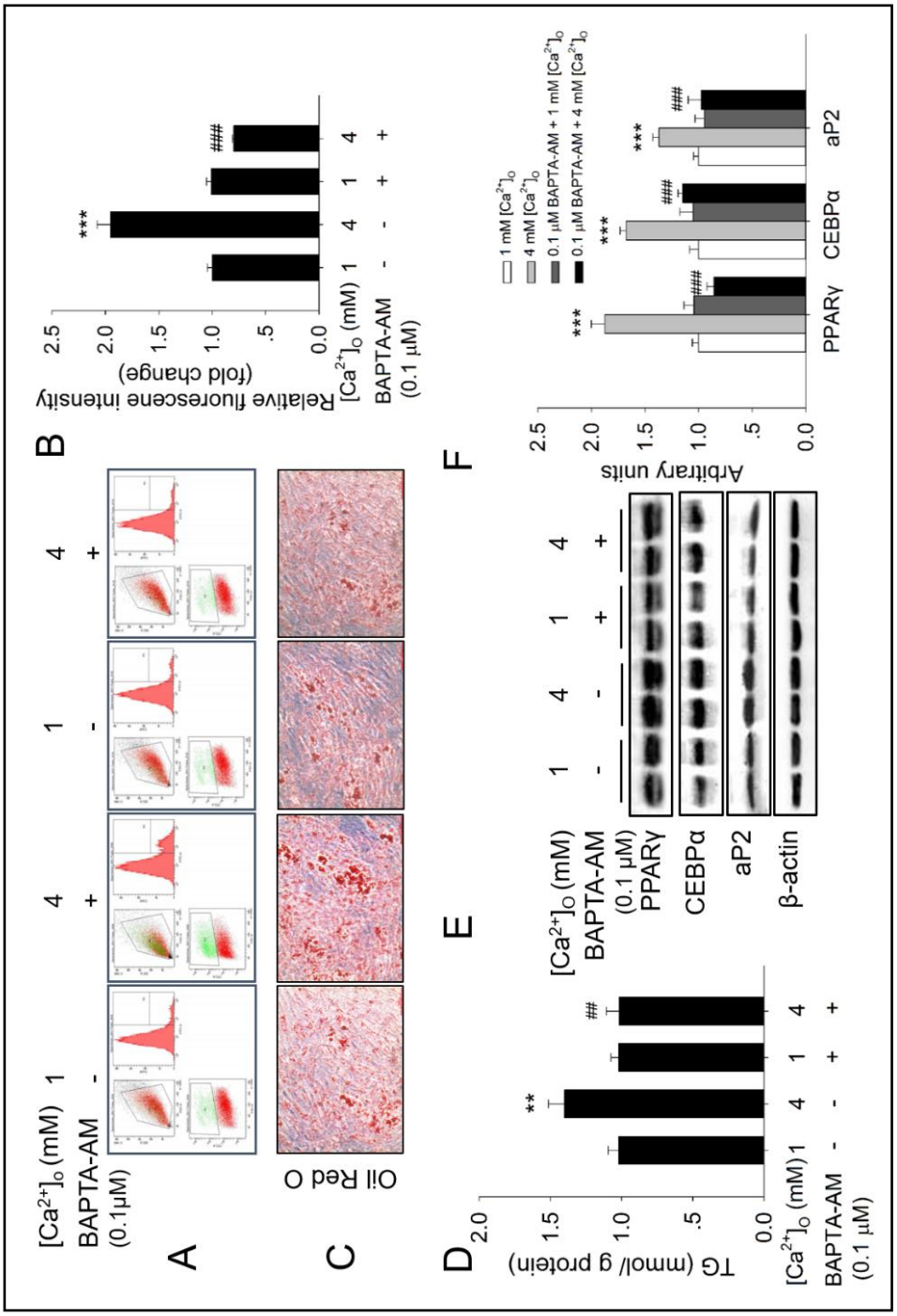

Fig. 3. Chelation of $[Ca^{2+}]_i$ prevented the $[Ca^{2+}]_o$-stimulated pBMSCs adipogenesis. A: $[Ca^{2+}]_i$ was analyzed by flow cytometry in the presence of 4 mM $[Ca^{2+}]_o$ and/or 0.1 μM BAPTA-AM. In the upper left image, the x axis is the forward scatter area (FSC-A) and the y axis is the side scatter area (SSC-A). In the bottom left image, the x axis is the forward scatter area (FSC-A) and the y axis is fluorescein isothiocyanate area (FITC-A). In the upper right image, the x axis is fluorescein isothiocyanate area (FITC-A) and the y axis is the cell count according to the different fluorescence displayed by the x-axis. B: The relative FITC fluorescence intensity of gated positive cells. C and D: Oil Red O staining (C) and TG contents assay (D) were conducted in the differentiated pBMSCs after 10-day adipogenic differentiation. E: Western blot analysis of PPARγ, C/EBPα and aP2 in the differentiated pBMSCs after 10-day adipogenic differentiation, and β-actin was used as a loading control. F: Mean ± SEM of immunoblotting bands and the intensities of the bands were expressed as the arbitrary units. ** P<0.01 and ***P<0.001 versus 1 mM $[Ca^{2+}]_o$ group (control), ##P<0.01 and ###P<0.001 versus 4 mM $[Ca^{2+}]_o$ group.

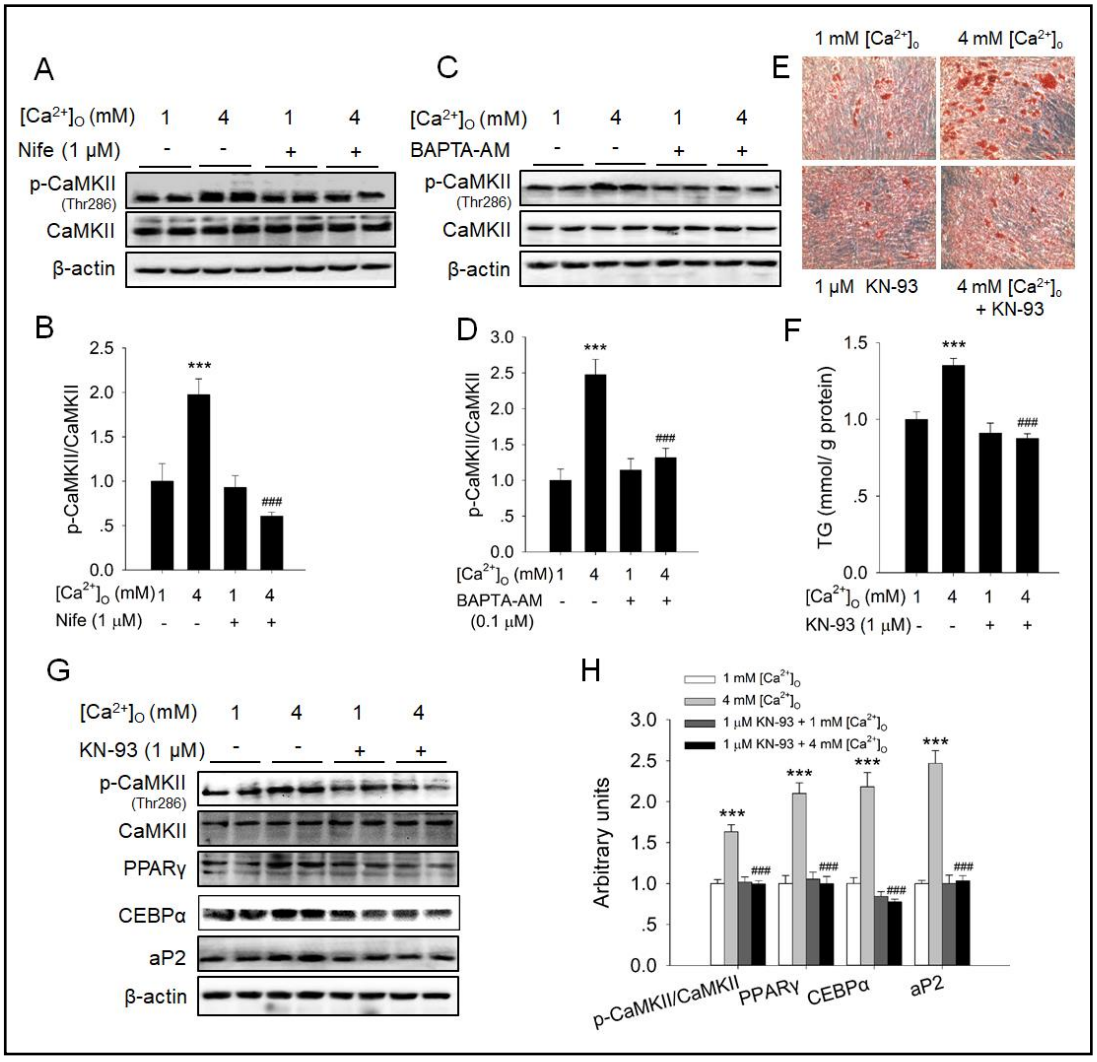

Fig. 4. Activation of CaMKII was involved in the $[Ca^{2+}]_o$-stimulated pBMSCs adipogenesis. A-D: Activation of CaMKII by $[Ca^{2+}]_o$ was reversed by Nifedipine (Nife) (A and B) and BAPTA-AM (C and D). A and C: Western blot analysis of p-CaMKII and CaMKII in the differentiated pBMSCs treated with 4 mM $[Ca^{2+}]_o$ and/or 1 μM Nife (A), and/or 0.1 μM BAPTA-AM (C) after 10-day adipogenic differentiation, and β-actin was used as a loading control. B and D: Mean ± SEM of immunoblotting bands of p-CaMKII/CaMKII, and the intensities of the bands were expressed as the arbitrary units. E-H: Inhibition of CaMKII signaling eliminated $[Ca^{2+}]_o$-stimulated adipogenesis of pBMSCs. E-F: Oil Red O staining (E) and TG contents assay (F) were conducted in the differentiated pBMSCs after 10-day adipogenic differentiation. G: Western blot analysis of p-CaMKII, CaMKII, PPARγ, C/EBPα and aP2, and β-actin was used as a loading control. H: Mean ± SEM of immunoblotting bands and the intensities of the bands were expressed as the arbitrary units. ***P<0.001 versus 1 mM $[Ca^{2+}]_o$ group (control), ###P<0.001 versus 4 mM $[Ca^{2+}]_o$ group.

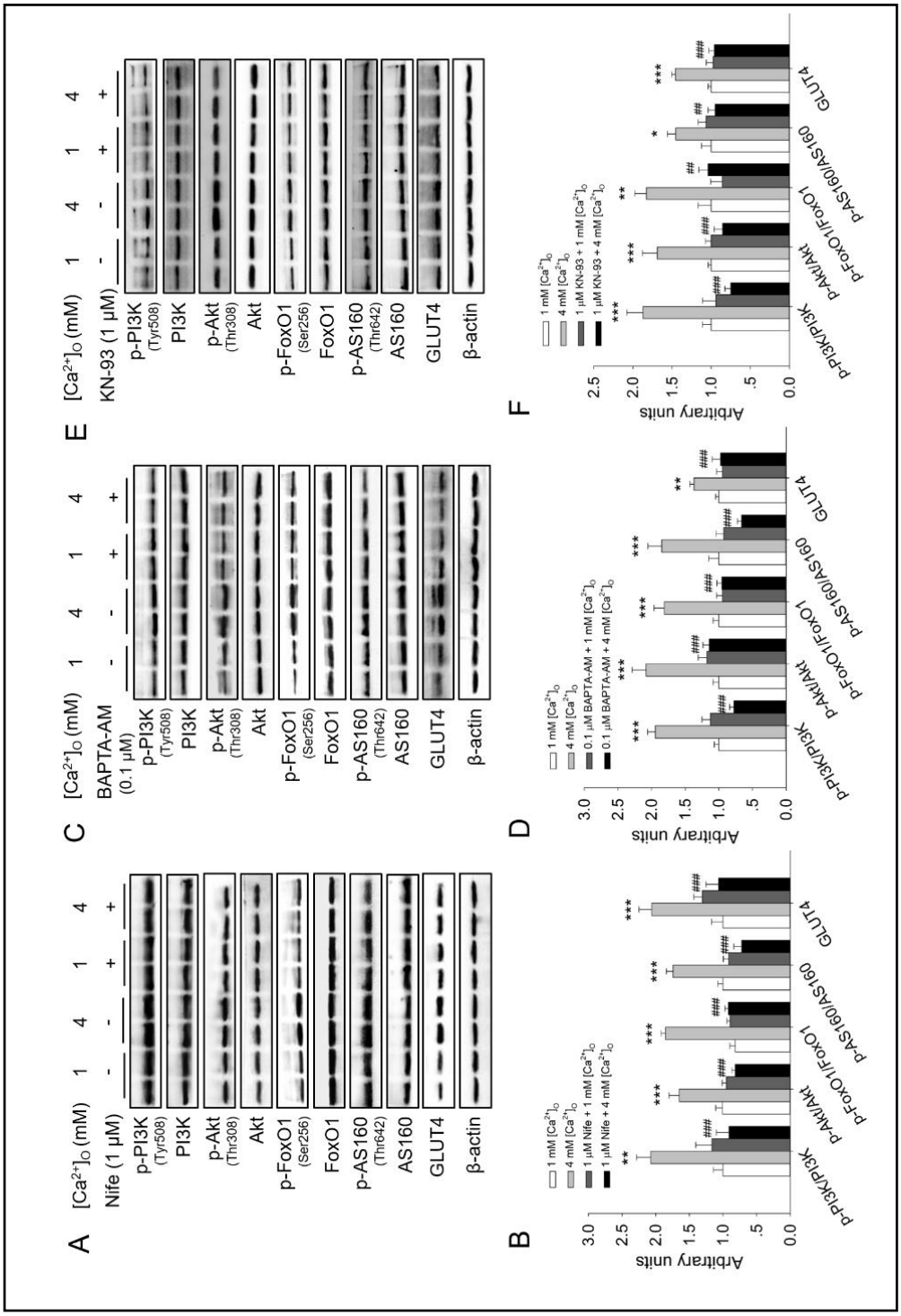

Fig. 5. $[Ca^{2+}]_o$-induced enhancement of PI3K/Akt signaling pathway depended on L-VGCC, $[Ca^{2+}]_i$ and CaMKII. A, C and E: Western blot analysis of p-PI3K, PI3K, p-Akt, Akt, p-FoxO1, FoxO1, p-AS160, AS-160 and GLUT4 in the differentiated pBMSCs treated with 4 mM $[Ca^{2+}]_o$ and/or 1 μM Nife (A), and/or 0.1 μM BAPTA-AM (C), and/or 1 μM KN-93 (E) after 10-day adipogenic differentiation. β-actin was used as a loading control. B, D and F: Mean ± SEM of immunoblotting bands and the intensities of the bands were expressed as the arbitrary units. * P<0.05, ** P<0.01 and ***P<0.001 versus 1 mM $[Ca^{2+}]_o$ group (control), ##P<0.01 and ###P<0.001 versus 4 mM $[Ca^{2+}]_o$ group.

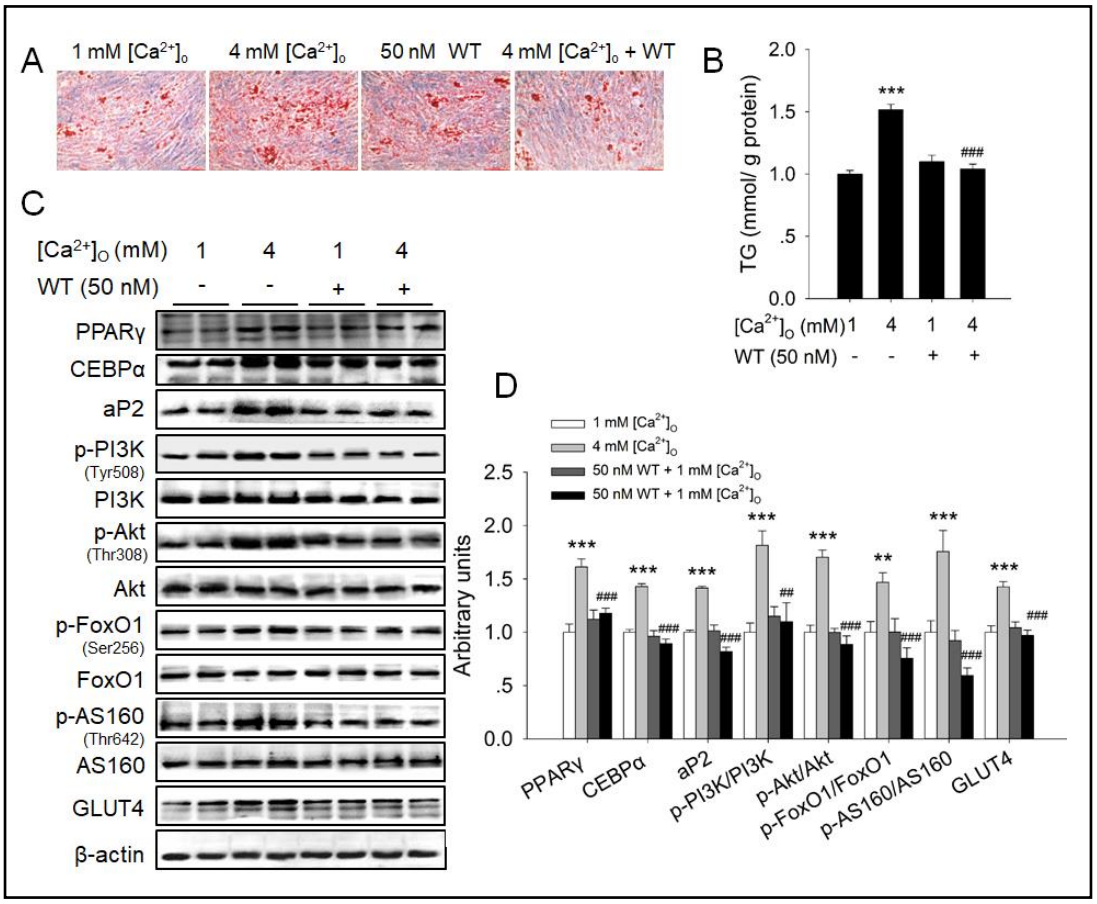

Fig. 6. Inhibition of PI3K/Akt signaling pathway abolished the $[Ca^{2+}]_o$-stimulated pBMSCs adipogenesis. A and B: Oil Red O staining (A) and TG contents assay (B) were conducted in the differentiated pBMSCs after 10-day adipogenic differentiation. C: Western blot analysis of PPARγ, C/EBPα, aP2, p-PI3K, PI3K, p-Akt, Akt, p-FoxO1, FoxO1, p-AS160, AS-160 and GLUT4 in the differentiated pBMSCs. β-actin was used as a loading control. D: Mean ± SEM of immunoblotting bands and the intensities of the bands were expressed as the arbitrary units. ** P<0.01 and ***P<0.001 versus 1 mM $[Ca^{2+}]_o$ group (control), ##P<0.01 and ###P<0.001 versus 4 mM $[Ca^{2+}]_o$ group.

Inhibition of PI3K/Akt signaling pathway abolished $[Ca^{2+}]_o$-stimulated pBMSCs adipogenesis

To further verify the effects of PI3K/Akt signaling pathway on $[Ca^{2+}]_o$-induced pBMSCs adipogenesis, Wortmannin (WT), a PI3K inhibitor, was applied to inhibit PI3K/Akt in the present study. As shown in Fig. 6A and B, the significant increase of lipid accumulation and TG content induced by 4 mM $[Ca^{2+}]_o$ were completely reversed by 50 nM WT. In addition, WT entirely abolished the $[Ca^{2+}]_o$-induced increase of p-PI3K/PI3K, p-Akt/Akt and p-FoxO1/FoxO1 ratios (Fig. 6C, D). Furthermore, the elevated expression of PPARγ, CEBPα, and aP2 in response to 4 mM $[Ca^{2+}]_o$ was fully eliminated by WT (Fig. 6C, D). These findings strongly suggested that the enhancement of PI3K/Akt-FoxO1 signaling pathway was responsible for the $[Ca^{2+}]_o$-stimulated pBMSCs adipogenesis.

$[Ca^{2+}]_o$ increased glucose uptake and utilization, GLUT4 expression and translocation through activation of CaMKII-PI3K/Akt-AS160 pathway

We also examined the effects of $[Ca^{2+}]_o$ on glucose uptake and utilization during pBMSCs adipogenesis. The result of 2-NBDG uptake assay showed that $[Ca^{2+}]_o$ significantly increased glucose uptake in the differentiated pBMSCs (Fig. 7A). Meanwhile, the glucose utilization

Fig. 7. $[Ca^{2+}]_o$ increased glucose uptake and utilization, GLUT4 expression and translocation through activation of CaMKII-PI3K/Akt-AS160 pathway. A: Effect of Nife, BAPTA-AM, KN-93 and WT on the increase of glucose uptake induced by $[Ca^{2+}]_o$. The 2-NBDG uptake were assayed in the differentiated pBMSCs after 10-day adipogenic differentiation. B and C: Western blot analysis of GLUT4 in the membrane (Mem-) and the cytoplasm (Cyt-) of the differentiated pBMSCs treated with 4 mM $[Ca^{2+}]_o$ and/or 1 μM Nife, and/or 0.1 μM BAPTA-AM (B), and/or 1 μM KN-93, and/or 50 nM WT (C) after 10-day adipogenic differentiation. Caveolin-1 and β-actin were used as the loading control of membrane protein and cytoplasm protein, respectively. D, E, F and G: Mean ± SEM of immunoblotting bands of Mem-GLUT4 and Cyt-GLUT4. The intensities of the Mem-GLUT4 bands were normalized to Caveolin-1 (D, F) and the intensities of the Cyt-GLUT4 bands were normalized to β-actin (E, G). ** P<0.01 and ***P<0.001 versus 1 mM $[Ca^{2+}]_o$ group (control), ##P<0.01 and ###P<0.001 versus 4 mM $[Ca^{2+}]_o$ group.

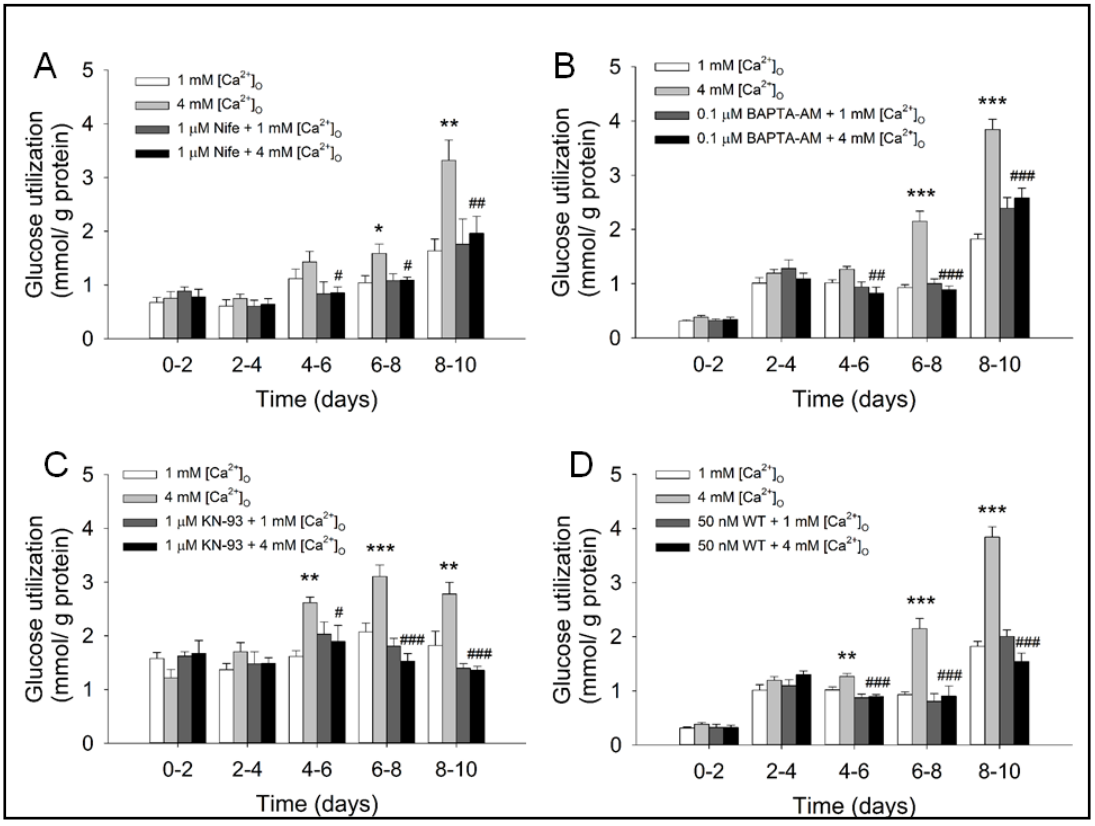

Fig. 8. Increase of glucose utilization induced by $[Ca^{2+}]_o$ is abolished by VGCC blocker Nifedipine, $[Ca^{2+}]_i$ chelator BAPTA-AM, CaMKII inhibitor KN-93 and PI3K/Akt inhibitor WT. A-D: Effect of Nifedipine (Nife) (A), BAPTA-AM (B), KN-93 (C) and Wortmannin (WT) (D) on the increase of glucose utilization induced by $[Ca^{2+}]_o$. Culture medium were changed every other day and were collected on days 2, 4, 6, 8 and 10 of differentiation. Meanwhile, the adipogenic medium without cells (un-culture medium) were also incubated and collected on the same day. Glucose utilization of cells was determined by subtracting the glucose content of the culture medium from that of the un-culture medium. The glucose contents were normalized to the corresponding protein content of cells.

assay revealed that, at the late stage (6-10 day) of differentiation, $[Ca^{2+}]_o$ induced remarkable elevation of glucose utilization (Fig. 8). In agreement with the $[Ca^{2+}]_o$-induced increase of glucose uptake and utilization, we found that $[Ca^{2+}]_o$ significantly enhanced GLUT4 expression (Fig. 5 and Fig. 6C, D) and translocation, with a significant increase of membrane GLUT4 expression and a remarkable decrease of cytoplasm GLUT4 expression in the differentiated pBMSCs (Fig. 7B-G). Furthermore, the phosphorylation level of AS160 (a substrate of Akt) in the differentiated pBMSCs was elevated by $[Ca^{2+}]_o$ (Fig. 5 and Fig. 6C, D). However, the increases of glucose uptake and utilization, the stimulation of GLUT4 expression and translocation, and the elevation p-AS160/AS160 ratio were abolished by L-VGCC blocker Nifedipine, $[Ca^{2+}]_i$ chelator BAPTA-AM, CaMKII inhibitor KN-93, and PI3K inhibitor WT (Fig. 6, Fig. 7 and Fig. 8). These results suggested that calcium influx via L-VGCC, elevation of $[Ca^{2+}]_i$ and activation of CaMKII-PI3K/Akt-AS160 signaling pathway were involved in $[Ca^{2+}]_o$-enhanced glucose uptake and utilization, GLUT4 expression and translocation during pBMSCs adipogenesis.

Calcium supplementation decreased body weight and fat content, while increased adipocyte number of iWAT in mice fed HFD

We further explored the effects of calcium supplementation on adipogenesis in mice fed HFD by determining the adipocyte number in iWAT. In this study, we found that calcium

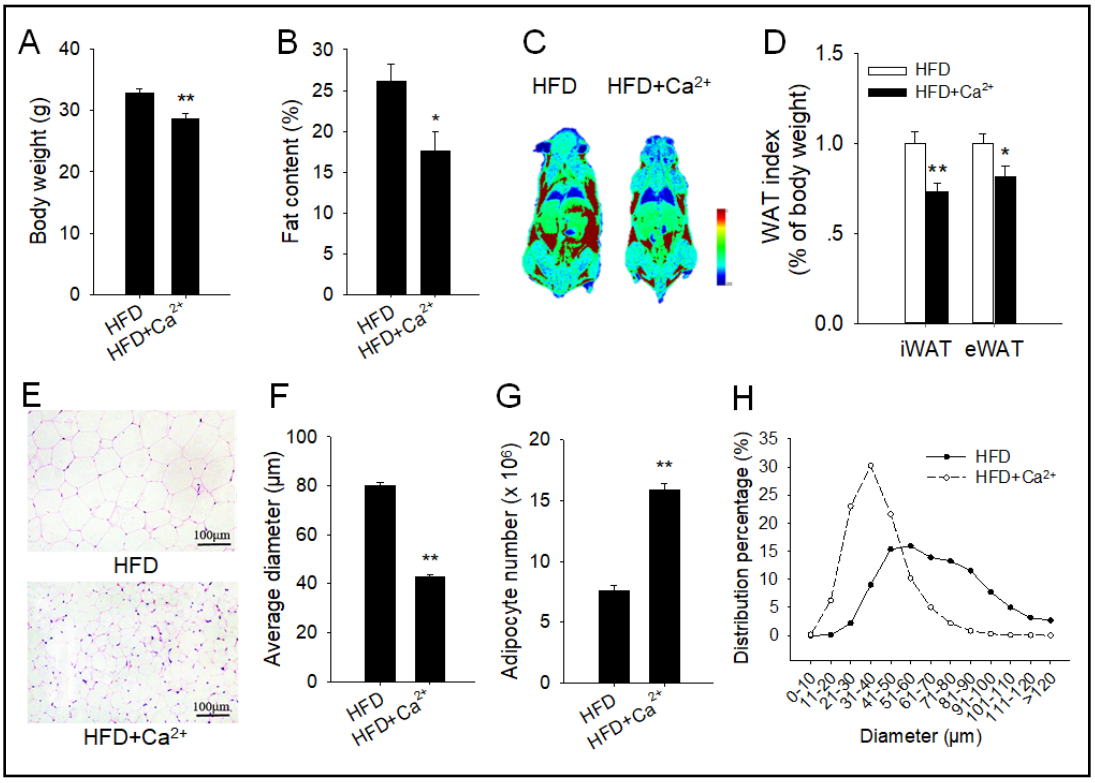

Fig. 9. Calcium supplementation decreased body weight and fat content, while increased adipocyte number of iWAT in mice fed HFD. A and B: Effects of calcium supplementation on body weight (A) and fat content (B). C: Fat distribution was analyzed in mice of HFD and HFD+Ca^{2+} groups. D: iWAT and eWAT index in mice of HFD and HFD+Ca^{2+} groups. E: H&E staining of mice iWAT. Scale bar, 100 μm. F: The average diameter of the adipocytes in iWAT of HFD and calcium-treated mice. G: The calculated adipocyte number in iWAT of HFD and calcium-treated mice. H: Distribution percentage of adipocyte diameter in of HFD and calcium-treated mice. * P<0.05 and **P<0.01 versus the HFD group.

supplementation in water significantly decreased body weight (Fig. 9A), with no effect on the average food intake (data not shown). Meanwhile, QMR results revealed that calcium supplementation led to a significant reduction of body fat content (Fig. 9B and C). Accordingly, the iWAT and eWAT index was also markedly decreased by calcium supplementation (Fig. 9D). In addition, H&E staining results showed that calcium supplementation resulted in the smaller adipocyte size (Fig. 9E), with the significant reduced average diameter in iWAT (Fig. 9F). Inspection of the diameter distribution indicated that diameter of most adipocytes (about 75%) in the HFD group was in the range of 40-100 μm. In contrast, diameter of most adipocytes (about 85%) in the calcium-supplemented group was in the range of 20-60 μm (Fig. 9H). Based on the average diameter of adipocyte in iWAT and the weight of iWAT, we calculated the total number of adipocytes in iWAT. Interestingly, our results demonstrated that calcium supplementation significantly increased adipocyte number in iWAT (Fig. 9G), suggesting that calcium supplementation enhanced adipogenesis or hyperplasia in mice iWAT.

Calcium supplementation improved glucose homeostasis, enhanced PPARγ and GLUT4 expression, and activated PI3K/Akt signaling pathway

To further investigate the effects of calcium supplementation on glucose homeostasis *in vivo*, we measured the blood glucose and serum insulin levels, and evaluated glucose tolerance and insulin sensitivity by performing OGTT and ITT in mice. As shown in Fig. 10A and B, blood glucose and serum insulin levels were significantly decreased in calcium-

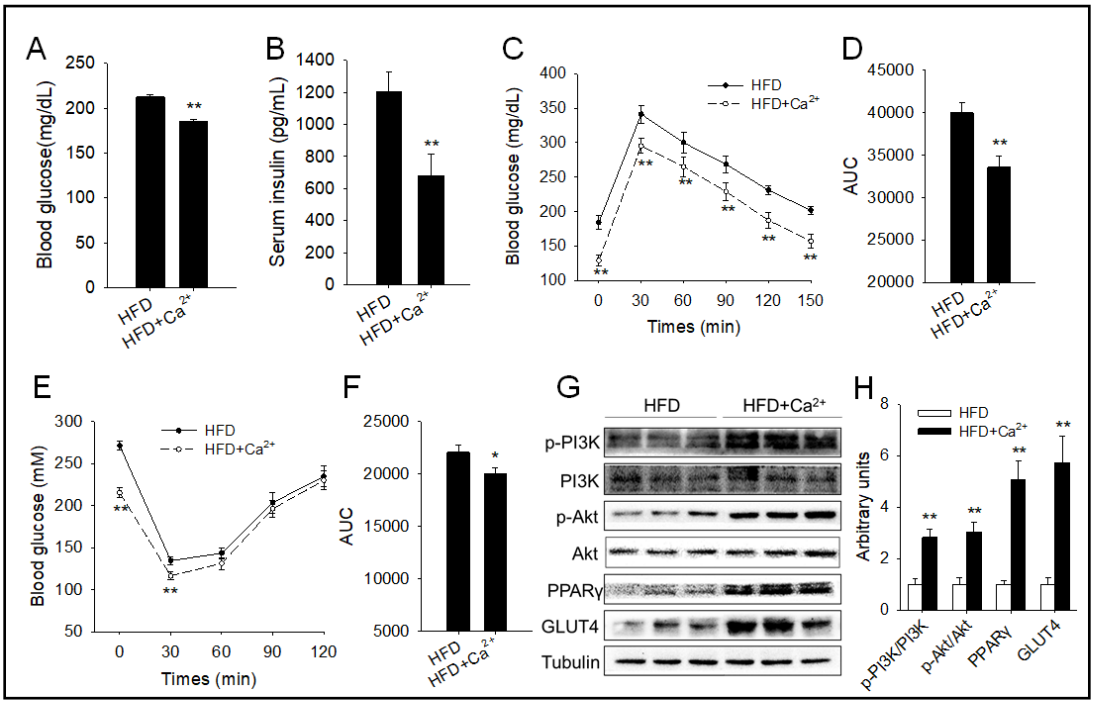

Fig. 10. Calcium supplementation improved glucose homeostasis, enhanced PPARγ and GLUT4 expression, and activated PI3K/Akt signaling pathway. A and B: Effects of calcium supplementation on the levels of blood glucose (A) and serum insulin (B). C: OGTT was performed in 4 h-fasted mice and the blood glucose concentration was measured. D: The area under the curve (AUC) of OGTT. E: ITT was performed in 4 h-fasted mice and blood glucose was detected. F: The AUC of ITT. G: Western blotting analysis of PI3K/Akt signaling and marker genes involved in adipogenesis (PPARγ) and glucose uptake (GLUT4). Tubulin was used as the loading control. H: Mean ± SEM of immunoblotting bands and the intensities of these proteins were expressed as arbitrary units. * P<0.05 and **P<0.01 versus the HFD group.

supplemented mice. In addition, calcium-treated mice exhibited improved glucose tolerance compared with HFD mice (Fig. 10C and D). Similarly, calcium-treated mice showed increased insulin sensitivity compared with HFD mice (Fig. 10E and F). Thus, our results indicated that calcium supplementation improved glucose homeostasis in mice fed HFD.

In consistent with the elevated adipocyte number or enhanced adipogenesis, and the improved glucose homeostasis induced by calcium supplementation, we found that calcium treatment significantly increased the expression of PPARγ and GLUT4 (Fig. 10G and H). Meanwhile, the ratios of p-PI3K/PI3K and p-Akt/Akt were markedly elevated by calcium treatment, indicating the activation of PI3K/Akt signaling pathway. These results suggested that activation of PI3K/Akt signaling pathway and subsequent enhanced expression of PPARγ and GLUT4 in iWAT might be involved in the increased adipocyte number and improved glucose homeostasis induced by calcium supplementation.

Discussion

In this paper, our results demonstrated that calcium supplementation enhanced adipogenesis and glucose uptake in pBMSCs, as well as increased adipocyte number and improved glucose tolerance and insulin sensitivity in HFD-fed mice, which might contribute to the calcium-induced body weight/fat reduction and glucose homeostasis improvement. It has been indicated that high $[Ca^{2+}]_o$ (9 mM) enhances adipocyte accumulation in mice BMSCs [12, 26] and that 5 mM $[Ca^{2+}]_o$ stimulates adipogenesis of porcine synovium-derived MSCs [27]. In line with these results, we found that $[Ca^{2+}]_o$ (4 mM) significantly promoted

pBMSCs adipogenesis through increasing the expression of adipogenic marker genes such as PPARγ, C/EBPα, and aP2. However, it has also been reported that high $[Ca^{2+}]_o$ (5 and 10 mM) attenuated adipogenesis in 3T3-L1 preadipocytes by inhibiting the expression of PPARγ and C/EBPα [28]. The inconsistent effects of $[Ca^{2+}]_o$ on adipogenesis were probably due to the different cell types and culture systems.

In agreement with the enhanced adipogenesis in pBMSCs, we found that calcium supplementation stimulated adipogenesis in mice fed HFD, with increased adipocyte number and PPARγ expression in iWAT. Similarly, dietary calcium propionate supplementation in finishing steers triggered upregulation of PPARγ mRNA expression level, which could cause long-term activation of adipogenesis [29]. Although the adipocyte number is increased, the adipocyte diameter/size in calcium-supplemented mice was much smaller than that of HFD mice. As a result, the WAT index, body fat content and body weight were significantly reduced by calcium supplementation, which was in line with the body weight/fat-lowering effects of calcium supplementation in the dietary obese mice [20, 21, 30] and human [31]. In contrast, it was also reported that increasing dairy calcium intake had no effect on decreasing body weight/fat of adolescent girls [32]. The discrepancy effects of calcium on body weight/fat loss might result from the different subjects, calcium intake amounts, and calcium intake periods.

It has been indicated that L-VGCC, an important calcium influx channel in the plasma membrane, is involved in $[Ca^{2+}]_o$-mediated adipogenesis of mice primary preadipocytes [33]. Similarly, we found that L-VGCC blocker Nifidipine prevented the increase of $[Ca^{2+}]_i$ and stimulation of pBMSCs adipogenesis induced by $[Ca^{2+}]_o$, therefore indicating the essential role of L-VGCC in this process. In addition, chelation of $[Ca^{2+}]_i$ with BAPTA-AM totally eliminated $[Ca^{2+}]_o$-induced increase of $[Ca^{2+}]_i$ and stimulation of pBMSCs adipogenesis, suggesting the involvement of elevated $[Ca^{2+}]_i$ in this process.

In agreement, increased $[Ca^{2+}]_i$ was found to promote adipogenesis of mice BMSCs [12, 26] and to boost the late stage of differentiation and lipid filling in human adipocyte differentiation [34]. Conversely, it was shown that chelation of $[Ca^{2+}]_i$ with BAPTA-AM caused a dramatic increase of adipogenesis in L7 cells [35]. The differences of cell types and culture system likely in part contributed to the discrepancies between the aforementioned studies.

CaMKII, an important mediator of $[Ca^{2+}]_i$ signaling in cell, can be activated by increased $[Ca^{2+}]_i$ [36]. In agreement, we found the increased $[Ca^{2+}]_i$ in response to $[Ca^{2+}]_o$ activated CaMKII, which was completely reversed by L-VGCC blocker and $[Ca^{2+}]_i$ chelator. In addition, inhibition of CaMKII totally blocked the $[Ca^{2+}]_o$-stimulated pBMSCs adipogenesis. Consistently, Szabo et al. reported a significant decrease of lipid accumulation and lower expression of adipogenic marker genes upon CaMKII inhibition in L7 cells [35]. Thus, our results strongly suggested that activation of CaMKII was involved in $[Ca^{2+}]_o$-stimulated pBMSCs adipogenesis.

The PI3K/Akt-FoxO1 signaling pathway plays a crucial role in the regulation of adipogenesis by enhancing the expression of adipogenic genes PPARγ and C/EBPα [37]. To be in accord, we found that $[Ca^{2+}]_o$ activated PI3K/Akt-FoxO1 signaling pathway in pBMSCs and calcium supplementation activated PI3K/Akt in mice iWAT, with the stimulation of pBMSCs adipogenesis and increase of adipocyte number. Additionally, the $[Ca^{2+}]_o$-activated PI3K/Akt-FoxO1 was abrogated by CaMKII inhibitor KN-93, while inhibition of PI3K had no significant influence on the phosphorylation of CaMKII (data not shown), suggesting that PI3K/Akt-FoxO1 pathway was the downstream of CaMKII. Furthermore, the activation of PI3K/Akt-FoxO1 induced by $[Ca^{2+}]_o$ was also blocked by L-VGCC inhibition and $[Ca^{2+}]_i$ chelation. Moreover, inhibition of PI3K prevented the $[Ca^{2+}]_o$-promoted pBMSCs adipogenesis. Collectively, these findings suggested that $[Ca^{2+}]_o$ influx via L-VGCC, elevation of $[Ca^{2+}]_i$, activation of CaMKII and subsequent enhancement of PI3K/Akt-FoxO1 signaling cascade were involved in the $[Ca^{2+}]_o$-stimulated pBMSCs adipogenesis.

Besides the regulatory effects on adipogenesis, calcium has also been implicated in the modulation of glucose uptake in 3T3-L1 cells [15]. In consistent, we found that $[Ca^{2+}]_o$ profoundly stimulated the 2-NBDG uptake and glucose utilization in the differentiated pBMSCs. Meanwhile, our results showed that calcium supplementation significantly reduced blood

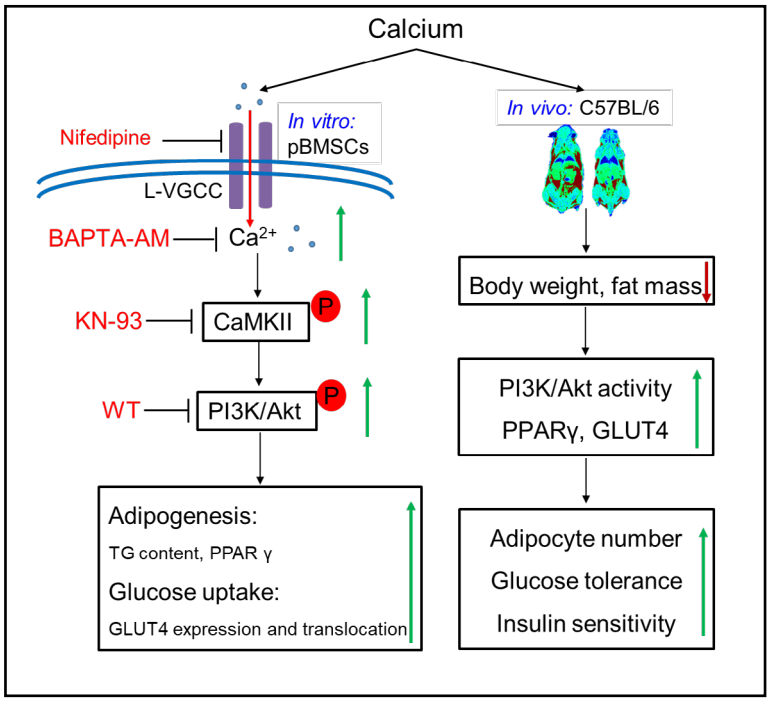

Fig. 11. Schematic representation of the mechanisms underlying the enhanced adipogenesis and improved glucose homeostasis induced by calcium supplementation. In vitro, $[Ca^{2+}]_o$ stimulated pBMSCs adipogenesis and glucose uptake by increasing $[Ca^{2+}]_i$, activating CaMKII and PI3K/Akt, and enhancing PPARγ and GLUT4 expression and GLUT4 translocation. In vivo, calcium supplementation decreased body weight and fat content, increased adipocyte number in iWAT, and improved glucose tolerance and insulin sensitivity, with elevated PPARγ and GLUT4 expression and PI3K/Akt activation.

glucose and serum insulin levels, and improved glucose tolerance and insulin sensitivity in HFD-fed mice. Similarly, the beneficial effects of dietary calcium on glycemic control has been indicated in many studies [16, 18, 38]. However, consumption of high calcium provided no effect on glycemic control in overweight patients with type 2 diabetes [17].

It has been well defined that PI3K/Akt signaling plays a key role in the regulation of glucose uptake [39], which involves the phosphorylation of AS160 [40] and translocation of GLUT4. In this study, we observed that $[Ca^{2+}]_o$ led to the enhancement of PI3K/Akt activation, AS160 phosphorylation, and GLUT4 expression and translocation from cytoplasm to cell membrane in the differentiated pBMSCs. Meanwhile, calcium supplementation activated PI3K/Akt and enhance GLUT4 expression in mice iWAT. In addition, the $[Ca^{2+}]_o$-stimulated of glucose uptake/utilization, AS160 phosphorylation, and GLUT4 expression and translocation were completely blocked by the PI3K inhibitor Wortmannin. Similarly, it was reported that PI3K/Akt was also involved in ursolic acid-stimulated AS160 phosphorylation, GLUT4 expression and translocation, and glucose uptake in 3T3-L1 adipocytes [41]. Moreover, we observed that PI3K/Akt-mediated AS160 phosphorylation, GLUT4 expression and translocation, and glucose uptake were also eliminated by L-VGCC inhibitor nifedipine, $[Ca^{2+}]_i$ chelator BAPTA-AM, and CaMKII inhibitor KN-93, suggesting the essential role of L-VGCC, $[Ca^{2+}]_i$ and CaMKII in this process. Similarly, it was reported that rutin-induced glucose uptake in rat soleus muscle was blunted by nifedipine and KN-93 [42]. At the same time, chelation of $[Ca^{2+}]_i$ with BAPTA-AM resulted in the inhibition of insulin-stimulated GLUT4 translocation and glucose uptake in 3T3-L1 cells [15]. Together, these data implied that $[Ca^{2+}]_o$ influx through L-VGCC, elevation of $[Ca^{2+}]_i$, activation of CaMKII and subsequent enhancement of PI3K/Akt-AS160 signaling cascade might be responsible for $[Ca^{2+}]_o$-induced GLUT4 translocation and glucose uptake in the differentiated pBMSCs and improved glucose homeostasis in HFD-fed mice.

Conclusion

Our findings suggested that calcium supplementation enhanced adipogenesis and glucose uptake in pBMSCs, which was coincident with the increased adipocyte number and improved glucose homeostasis in HFD-fed mice, and was associated with activation

of CaMKII and PI3K/Akt-FoxO1/AS160 signaling pathway (Fig. 11). These data provide a broader understanding of the mechanisms underlying dietary calcium-induced body weight loss and glycemic control and help to develop nutritional intervention/therapy strategies for obesity, insulin resistance and related type 2 diabetes.

Acknowledgements

This work was supported by the National Natural Science Foundation of China (31790411, 31372397, 31672508) and Guangdong special support program (2014TQ01N260).

Disclosure Statement

The authors have declared no conflicts of interest.

References

1 Seidell JC, Halberstadt J: The global burden of obesity and the challenges of prevention. Annals of nutrition & metabolism 2015;66 Suppl 2:7-12.
2 Rutkowski JM, Stern JH, Scherer PE: The cell biology of fat expansion. J Cell Biol 2015;208:501-512.
3 Choe SS, Huh JY, Hwang IJ, Kim JI, Kim JB: Adipose Tissue Remodeling: Its Role in Energy Metabolism and Metabolic Disorders. Frontiers in endocrinology 2016;7:30.
4 Smith U, Kahn BB: Adipose tissue regulates insulin sensitivity: role of adipogenesis, de novo lipogenesis and novel lipids. Journal of internal medicine 2016;280:465-475.
5 Wang J, Hu X, Ai W, Zhang F, Yang K, Wang L, Zhu X, Gao P, Shu G, Jiang Q, Wang S: Phytol increases adipocyte number and glucose tolerance through activation of PI3K/Akt signaling pathway in mice fed high-fat and high-fructose diet. Biochemical and biophysical research communications 2017;489:432-438.
6 Tang QQ, Lane MD: Adipogenesis: from stem cell to adipocyte. Annual review of biochemistry 2012;81:715-736.
7 Padilla-Benavides T, Velez-delValle C, Marsch-Moreno M, Castro-Munozledo F, Kuri-Harcuch W: Lipogenic Enzymes Complexes and Cytoplasmic Lipid Droplet Formation During Adipogenesis. J Cell Biochem 2016;117:2315-2326.
8 Moraes-Vieira PM, Saghatelian A, Kahn BB: GLUT4 Expression in Adipocytes Regulates De Novo Lipogenesis and Levels of a Novel Class of Lipids With Antidiabetic and Anti-inflammatory Effects. Diabetes 2016;65:1808-1815.
9 Swindle MM, Makin A, Herron AJ, Clubb FJ, Jr., Frazier KS: Swine as models in biomedical research and toxicology testing. Vet Pathol 2012;49:344-356.
10 Jensen B, Farach-Carson MC, Kenaley E, Akanbi KA: High extracellular calcium attenuates adipogenesis in 3T3-L1 preadipocytes. Experimental cell research 2004;301:280-292.
11 Shi H, Halvorsen YD, Ellis PN, Wilkison WO, Zemel MB: Role of intracellular calcium in human adipocyte differentiation. Physiological genomics 2000;3:75-82.
12 Hashimoto R, Katoh Y, Miyamoto Y, Itoh S, Daida H, Nakazato Y, Okada T: Increased extracellular and intracellular Ca(2)(+) lead to adipocyte accumulation in bone marrow stromal cells by different mechanisms. Biochemical and biophysical research communications 2015;457:647-652.
13 Zechner C, Beyersdorf F, Doenst T: The role of calcium in the regulation of glucose uptake in isolated working rat heart. Molecular and cellular biochemistry 2002;232:75-80.
14 Lanner JT, Katz A, Tavi P, Sandstrom ME, Zhang SJ, Wretman C, James S, Fauconnier J, Lannergren J, Bruton JD, Westerblad H: The role of Ca2+ influx for insulin-mediated glucose uptake in skeletal muscle. Diabetes 2006;55:2077-2083.
15 Whitehead JP, Molero JC, Clark S, Martin S, Meneilly G, James DE: The role of Ca2+ in insulin-stimulated glucose transport in 3T3-L1 cells. The Journal of biological chemistry 2001;276:27816-27824.

16 Gomes JM, Costa JA, Alfenas RC: Could the beneficial effects of dietary calcium on obesity and diabetes control be mediated by changes in intestinal microbiota and integrity? The British journal of nutrition 2015;114:1756-1765.
17 Gomes JMG, Costa JdA, Alfenas RdCG: Dietary calcium from dairy, body composition and glycaemic control in patients with type 2 diabetes pursuing an energy restricted diet: A parallel group randomised clinical trial. International Dairy Journal 2017;73:50-56.
18 Thomas AP, Dunn TN, Drayton JB, Oort PJ, Adams SH: A dairy-based high calcium diet improves glucose homeostasis and reduces steatosis in the context of preexisting obesity. Obesity (Silver Spring, Md) 2013;21:E229-235.
19 Soares MJ, Pathak K, Calton EK: Calcium and vitamin D in the regulation of energy balance: where do we stand? International journal of molecular sciences 2014;15:4938-4945.
20 Sergeev IN, Song Q: High vitamin D and calcium intakes reduce diet-induced obesity in mice by increasing adipose tissue apoptosis. Mol Nutr Food Res 2014;58:1342-1348.
21 Chaplin A, Parra P, Laraichi S, Serra F, Palou A: Calcium supplementation modulates gut microbiota in a prebiotic manner in dietary obese mice. Mol Nutr Food Res 2016;60:468-480.
22 DU M-q, HUANG Y-q, Nai-Sheng L, Gang S, ZHU X-t, WANG L-n, Ping G, XI Q-y, ZHANG Y-l, WANG S-b: Characterization and differentiation into adipocytes and myocytes of porcine bone marrow mesenchymal stem cells. Journal of Integrative Agriculture 2014;13:837-848.
23 Wang S, Liang X, Yang Q, Fu X, Rogers CJ, Zhu M, Rodgers BD, Jiang Q, Dodson MV, Du M: Resveratrol induces brown-like adipocyte formation in white fat through activation of AMP-activated protein kinase (AMPK) alpha1. International journal of obesity (2005) 2015;39:967-976.
24 Villanueva Claudio J, Vergnes L, Wang J, Drew Brian G, Hong C, Tu Y, Hu Y, Peng X, Xu F, Saez E, Wroblewski K, Hevener Andrea L, Reue K, Fong Loren G, Young Stephen G, Tontonoz P: Adipose Subtype-Selective Recruitment of TLE3 or Prdm16 by PPARγ Specifies Lipid Storage versus Thermogenic Gene Programs. Cell metabolism 2013;17:423-435.
25 Ye J, Ai W, Zhang F, Zhu X, Shu G, Wang L, Gao P, Xi Q, Zhang Y, Jiang Q, Wang S: Enhanced Proliferation of Porcine Bone Marrow Mesenchymal Stem Cells Induced by Extracellular Calcium is Associated with the Activation of the Calcium-Sensing Receptor and ERK Signaling Pathway. Stem Cells International 2016;2016:1-11.
26 Hashimoto R, Katoh Y, Nakamura K, Itoh S, Iesaki T, Daida H, Nakazato Y, Okada T: Enhanced accumulation of adipocytes in bone marrow stromal cells in the presence of increased extracellular and intracellular [Ca(2)(+)]. Biochemical and biophysical research communications 2012;423:672-678.
27 Dry H, Jorgenson K, Ando W, Hart DA, Frank CB, Sen A: Effect of calcium on the proliferation kinetics of synovium-derived mesenchymal stromal cells. Cytotherapy 2013;15:805-819.
28 Jensen B, Farach-Carson MC, Kenaley E, Akanbi KA: High extracellular calcium attenuates adipogenesis in 3T3-L1 preadipocytes. Experimental cell research 2004;301:280-292.
29 Zhang XZ, Meng QX, Lu L, Cui ZL, Ren LP: The effect of calcium propionate supplementation on performance, meat quality, and mRNA expression of finishing steers fed a high-concentrate diet. Journal of Animal and Feed Sciences 2015;24:100-106.
30 Sun C, Wang L, Yan J, Liu S: Calcium ameliorates obesity induced by high-fat diet and its potential correlation with p38 MAPK pathway. Molecular biology reports 2012;39:1755-1763.
31 Li P, Fan C, Lu Y, Qi K: Effects of calcium supplementation on body weight: a meta-analysis. The American journal of clinical nutrition 2016;104:1263-1273.
32 Lappe JM, McMahon DJ, Laughlin A, Hanson C, Desmangles JC, Begley M, Schwartz M: The effect of increasing dairy calcium intake of adolescent girls on changes in body fat and weight. The American journal of clinical nutrition 2017;105:1046-1053.
33 Sun C, Qi R, Wang L, Yan J, Wang Y: p38 MAPK regulates calcium signal-mediated lipid accumulation through changing VDR expression in primary preadipocytes of mice. Molecular biology reports 2012;39:3179-3184.
34 Shi H, Halvorsen Y-D, Ellis PN, Wilkison WO, Zemel MB: Role of intracellular calcium in human adipocyte differentiation. Physiological genomics 2000;3:75-82.
35 Szabo E, Qiu Y, Baksh S, Michalak M, Opas M: Calreticulin inhibits commitment to adipocyte differentiation. The Journal of cell biology 2008;182:103-116.
36 Bootman MD: Calcium signaling. Cold Spring Harbor perspectives in biology 2012;4:a011171.

37 Shu G, Lu NS, Zhu XT, Xu Y, Du MQ, Xie QP, Zhu CJ, Xu Q, Wang SB, Wang LN, Gao P, Xi QY, Zhang YL, Jiang QY: Phloretin promotes adipocyte differentiation *in vitro* and improves glucose homeostasis *in vivo*. J Nutr Biochem 2014;25:1296-1308.

38 Asemi Z, Karamali M, Esmaillzadeh A: Effects of calcium-vitamin D co-supplementation on glycaemic control, inflammation and oxidative stress in gestational diabetes: a randomised placebo-controlled trial. Diabetologia 2014;57:1798-1806.

39 Saltiel AR, Kahn CR: Insulin signalling and the regulation of glucose and lipid metabolism. Nature 2001;414:799-806.

40 Miinea CP, Sano H, Kane S, Sano E, Fukuda M, Peranen J, Lane WS, Lienhard GE: AS160, the Akt substrate regulating GLUT4 translocation, has a functional Rab GTPase-activating protein domain. The Biochemical journal 2005;391:87-93.

41 He Y, Li W, Li Y, Zhang S, Wang Y, Sun C: Ursolic acid increases glucose uptake through the PI3K signaling pathway in adipocytes. PloS one 2014;9:e110711.

42 Kappel VD, Zanatta L, Postal BG, Silva FRMB: Rutin potentiates calcium uptake via voltage-dependent calcium channel associated with stimulation of glucose uptake in skeletal muscle. Archives of biochemistry and biophysics 2013;532:55-60.